Charge Transport Mechanism and Low Temperature Phase Transitions in KIO_3

M.M. Abdel Kader, F. El-Kabbany, H.M. Naguib and W.M. Gamal

Abstract Our report deals with the measurement of some electrical properties, namely the ac conductivity $\sigma(\omega, T)$ and the complex dielectric permittivity $\varepsilon^*(\omega, T)$ in the temperature interval 95 K < T < 280 K and at some selected frequencies (0.7–20 kHz) for polycrystalline samples of potassium iodate KIO_3 using a computerized RLC meter. The improper character of the ferroelectricity over the mentioned temperature range has been achieved by recording the ferroelectric hysteresis loops. The temperature dependence of each electrical parameter reveals that the compound undergoes two phase transitions at T ≈ 258 K and at T ≈ 110 K. The frequency dependent conductivity seems to be in accordance with the power law $\sigma(\omega, T)\alpha\omega^{S(T)}$ and the trend of temperature dependence of the frequency exponent s (0 < s < 1) suggests that the quantum mechanical tunneling (QMT) model is the main mechanism of the charge transport. Comparison with the behavior of the NH_4IO_3 in the same temperature range was outlined.

1 Introduction

Potassium iodate KIO_3 is a member of the monovalent metal iodate series of the general molecular formula MIO_3 where M stands for Li, Cs, Na, K… and/or NH_4. This series of compounds attracted the attention of investigators due to their interesting properties. For example, the improper ferroelectric hydrogen-bonded NH_4IO_3 undergoes a ferroelectric phase transition at ≈368 K [1–3]. Moreover, since the compound behaves as a proton conductor, therefore it has some practical applications such as chemical sensors, electrochromic displays and supercapacitors [3, 4]. Furthermore, $LiIO_3$ undergoes successive phase transitions and the high temperature phase behaves as a superionic conductor [5, 6]. Properties such as

M.M. Abdel Kader (✉) · F. El-Kabbany · H.M. Naguib · W.M. Gamal
Physics Department, Faculty of Science, Cairo University, Giza, Egypt
e-mail: m_m_abdelkader@yahoo.com

F.L. Gaol et al. (eds.), *Recent Trends in Physics of Material Science and Technology*,
Springer Series in Materials Science 204, DOI 10.1007/978-981-287-128-2_6

piezoelectric, pyroelectric and non-linear optical effects are common for some members of this series [7–11].

For KIO_3, which is the subject of this article, it is known that most of the physical properties of the crystals of this compound such as, (dc) dielectric constant [12] piezoelectric and pyroelectric effects [13, 14], electro-optical behavior [13], non-linear optical properties [7, 14], ferroelectricity [15, 16] in addition to nuclear quadruple resonance (NQR) [12] and Raman scattering experiment [17], have been investigated previously. Later on, some of these properties were discussed [18]. Due to the increasing interest of these properties and the expected applications of such a material in laser technology, it is logical to re-examine these properties using more advanced techniques. For example, a somewhat recent work dealing with the temperature dependence for piezoelectric and ferroelastic properties, using resonance—antiresonance method [19], has been reported. The data indicate that the compound undergoes successive five phase transitions (I–II, II–III, III–IV, IV–V, V–VI) at the transition temperatures: T_1 = 485 K, T_2 = 345.5 K, T_3 = 258 K, T_4 = 113 K and T_5 = 33 K respectively. Similar behavior was observed earlier [12] with somewhat slight different in the value of the transition temperature for some phases. The anomaly that has been observed around ≈150 °C (423 K) by Crane [14], Herlach [12], Maeda et al. [19] and more recently at (428 ± 2)K by the present authors [20] has been already explained as a change in electrical conduction between extrinsic and intrinsic mechanisms [20] and hence it is not related to any phase transition [19, 20].

Among other things, KIO_3 single crystal exhibits noble non-linear optical properties in all phases [7]. Furthermore, its non-linear optical coefficient in the room temperature phase (phase III), is the largest between monovalent metal iodates (MIO_3) [7, 21] and is also greater than those of KH_2PO_4 (KDP), BaB_2O_4 (BBO) and $LiBrO_5$ (LBO), which are known as double frequency materials in the ultraviolet wavelength [22]. Although the presence of ferroelectric domains and twins at room temperature (phase III) prevents or at least hinders practical applications, yet using the poling technique and specially after detwenning and domain removal, it can be used for fabrication of non-linear optical devices [22].

Another point of interest is that the static piezoelectric constants of the single crystals of KIO_3 in phase III are about 50 times greater than those of α-quartz [23]. Due to this large piezoelectric effect, KIO_3 is a promising candidate for the fabrication of piezoelectric sensors [24]. Furthermore, the thermal characterization including specific heat and thermal decomposition in the temperature interval 260 K < T < 600 K were investigated [25] using Perkin—Elmr DSC.

To clarify the dynamic properties of the high temperature phase transition of KIO_3 crystals, the temperature dependence of low frequency (soft) optical modes was measured by Raman scattering [24]. More recently, detailed polarized Raman study were performed on KIO_3 single crystals over 78.5–553 K [26]. The improper character of ferroelectricity of the compound was suggested by Ahart et al. [24], supported by Liu et al. [26] and confirmed by Abdel-Kader et al. [20].

From the accurate measurements of some mentioned properties as a function of temperature [15, 17, 19, 20, 22–25], it has been reported that, the KIO_3 undergoes a

ferroelectric phase transition around 486 K and several phase transitions as summarized in Table 1. The table shows also the symmetry of some phases of KIO_3

Regarding the crystal structure, it is known that the structure of phase III using the single crystal X-ray diffraction technique, was determined by Crane [14] who also summarized the results of studies on KIO_3 until 1971 [14]. Furthermore, based on X-ray powder diffraction data, Hamid [27] suggested the space group of phase I

Table 1 Summary of phase transitions in KIO_3

Phase transition	Symmetry	Transition temperature (TK)	Technique or property	References
I–II	I Rhombohederal (*R3 m*, *Z* = 1) [20] Rhombohederal (*R3*, *Z* = 1) [30] Rhombohederal $(R\bar{3}m,\ Z = 2)$ [18] Rhombohederal (*R3 m*, *Z* = 2) [17]	485 K	Raman Spectroscopy	[24]
			Elastic and piezoelectric	[19]
			Detewenning and domain removing procedure	[22]
			Ferroelectricity and optical properties.	[15]
		(486 ± 1) K	Ac conductivity	[20]
		487 K	Thermal properties	[25]
II–III	II Monoclinic (*Cm*, *Z* = 8) [18] Monoclinic (*Pm*, *Z* = 4) [17]	345 K	Raman Spectroscopy	[24]
			Ac conductivity	[20]
			Thermal properties	[25]
			Ferroelectricity and optical properties.	[15]
		345.5 K	Elastic and piezoelectric	[19]
		345.6 K	Elastic properties	[23]
		343 K	Detewenning and domain removing procedure	[22]
III–IV	III Triclinic (*P1*, *Z* = 4) [31] Triclinic (*P1*, *Z* = 4) [17] Triclinic (*P1*, *Z* = 4) [18]	258 K	Ac conductivity	Present work
			Raman Spectroscopy	[17]
			Elastic and piezoelectric	[19]
IV–V	_	110 K	Ac conductivity	Present work
			Raman Spectroscopy	[17]
		113 K	Elastic and piezoelectric	[19]
V–VI	_	33 K	Elastic and piezoelectric	[19]

as R3 m which has not been yet confirmed. He also suggested the symmetry of phase II and determined the structure of Phase I from intensities taken by photographic method. It is known that, single crystals X-ray diffraction technique, has been faced with the some problems due to the existence of ferroelectric and/or ferroelastic domains [27].

Again single crystal technique has been used by Kalinin et al. [28] and has been faced with the same problems namely the tendency towards twinning and polymorphism [28].

To overcome all these problems, recently Kasatani et al. [29] determined, the crystal structure of phase I at 530 K using high energy X-ray technique and the MEM/Rietveld analysis. On the other hand, the high resolution neutron powder diffraction has been employed for determination of the crystal structure of phase I at 523 K [30], and also phase III at 300 K [31], at 100 and 10 K [32].

We have found that it is of interest to measure the ac conductivity and dielectric permittivity in the low temperature range 95 K < T < 280 K on polycrystalline samples. This technique is absent in literature for the title compound. Another reason for the use of this technique in the present work is the dependence of the physico—chemical properties of this compound on the method of its recrystallization. For example, different NQR^{127} I spectra were found for crystals grown from water solution with or without HIO_3 [33]. Moreover, for crystallization of KIO_3 from an aqueous solution containing HIO_3 and KIO_3 with a ratio of HIO_3/KIO_3 greater than 7.4 %, crystals of KIO_3 and $KH(IO_3)_2$ are formed [23].

According to the best of our knowledge, no data on "electrical transport mechanism" in the investigated low temperature region was reported. Also the motivation behind the present work, is to compare our data with that of the very similar compound namely NH_4IO_3 [34].

In order to discuss the different models for conduction mechanism, the starting point is that, the total measured ac conductivity $\sigma_{ac(total)}$ at a given angular frequency (ω), can be separated into dc and ac components namely:

$$\sigma_{ac(total)} = \sigma_{dc} + \sigma_{(ac)} \tag{1}$$

The ac component $\sigma(\omega)$ is a function of both frequency (ω) and temperature (T) and may be written as $\sigma(\omega, T)$ whereas the dc component is a function of temperature only. According of Jonscher [35] $\sigma(\omega) \propto \omega^{s(T)}$, therefore

$$\sigma(\omega) = A(T)\omega^{s(T)} \tag{2}$$

This is the well known power law [35–43] and has been so widely observed for highly disordered materials and hence it has come to be known as a universal dynamic response.

The pre-factor A (T) is a constant and represents the degree of polarizability [38] and the frequency exponent s ($0 < s < 1$) describes the interaction (mainly of an electrostatic type) between the mobile ions with lattice around them or in more details, and according to the many body interaction model [35, 38], the interaction

between all dipoles participating in the polarization process is characterized by the parameter s. A unit value of s implies a pure Debye type interaction. The value of s decreases with the increase of interaction [38, 41]. The thermal behavior of the ac conductivity follows Arrhenius relation in most cases.

$$\sigma T = \sigma_o \exp(-E/kT) \tag{3}$$

where E is the activation energy for the process, k is the Boltzmann's constant and σ_o is constant.

Furthermore, it is known that the complex dielectric permittivity $\varepsilon^*(\omega, T)$ can be divided into the real part $\varepsilon'(\omega, T)$ and the imaginary part $\varepsilon''(\omega, T)$ according to the equation:

$$\varepsilon^*(\omega, T) = \varepsilon'(\omega, T) - j\varepsilon''(\omega, T) \tag{4}$$

(ε' and ε'' are frequency-dependent and represent the charging and loss currents respectively) [44].

2 Experimental Procedures

2.1 Sample Preparation

The material used in the present work was manufactured by the BDH Chemical Company Ltd. For electrical and/or ferroelectric measurements, a suitable amount of the fine polycrystalline powder of the compound, sufficient to prepare 5–6 pellets was further grained under 2 μm (micronized). The aim of this technique is to remove the effect of grain size and also to minimize the effect of porosity.

A microanalytical balance, type Sartorius, was used to achieve the equality of masses between all samples before compressing, (the mass of each sample was ≈0.6 gm). These samples were pressed under the same pressure (of about 2×10^8 N/m^2) so we have practically identical pellets of thickness ≈2 mm and of diameter ≈1 cm.
Good electrical contact was attained by painting the opposite faces of each pellet with air drying conducting silver paste. Before any measurements, the samples were inserted into a dessicator over night to remove any humidity. A sample holder with brass electrodes was specially designed to fit the present measurements.

2.2 Characterization Techniques

To demonstrate and to check the presence of ferroelectricity at different temperatures, the circuit shown in Fig. 1a, was designed and manufactured in the Science Technical Center, Cairo University to fit the present measurement. The digital

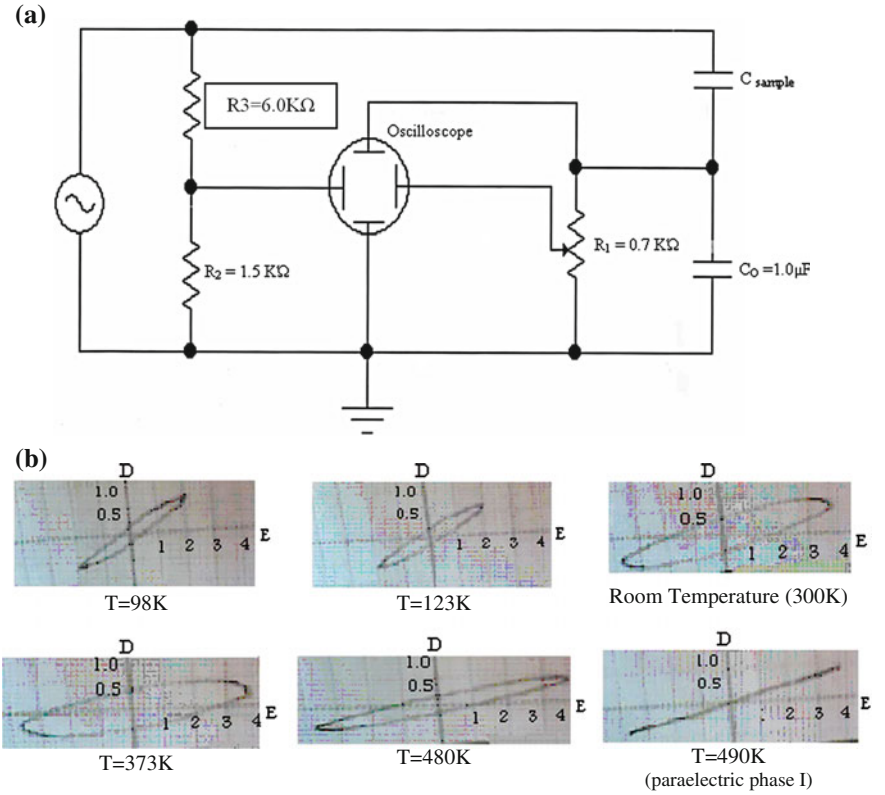

Fig. 1 **a** The designated circuit for detecting ferroelectric hysteresis loops. **b** The D-E hysteresis loops for KIO_3 (Arb. Scale)

storage oscilloscope type Instek GDS-820S, provided with a computerized camera as connected in the designated circuit shown was used to record ferroelectric hysteresis loops at different temperatures. Calibration, using triglycine sulphate (TGS), was carried out just before any actual run.

A computerized LCR bridge type Philips PM6304 was used to determine the ac conductivity and the dielectric permittivity at some selected frequencies. The bridge measures precisely the values of R, C, Z, Q… However, in the present work the values of R and C are converted into conductivity and permittivity using the dimensions of the pellet and a simple program, since the bridge is interfaced to computer. The dc conductivity was measured by using an electrometer, type Keithly 614. Data were collected on at least three virgin samples and the results were found to be quite consistent and reproducible. All measurements were performed during heating run. The heating rate was 0.5 K/min and the experimental error of temperature is better than +1 %. All measurements were performed at the thermal equilibrium. Calibration was done on a standard sample before any actual measurements.

3 Results

3.1 Ferroelectricity

The ferroelectric hysteresis loops (D-E loops) at some selected temperatures in the range 95 K < T < 280 K have been displayed and recorded on the monitor of the digital-storage oscilloscope. Two of these loops are shown in Fig. 1b, together with D-E loops recorded at high temperature up to 490 K where the compound is in the paraelectric phase. It seems likely that, the saturation in the D-E loops is not complete. This problem will be discussed later on (in the discussion section). The existence of this type of D-E loops is an indication that the compound behaves as an improper ferroelectric material.

3.2 Dielectric Permittivity

The temperature dependence (95 K < T< 280 K) of the real part ε′ of the dielectric permittivity determined at some selected frequencies (0.7–20 kHz) is shown in Fig. 2.

In general, the value of ε′ depends on both the frequency (f) and temperature (T). For a given frequency, each curve is characterized by the existence of two anomalies: a pronounced peak in the vicinity of $T_3 \approx 258$ K and a small peak (anomaly) at $T_4 \approx 110$ K. Between the two transition regions, the value of ε′ is almost temperature independent. It is known that, The compound undergoes a ferroelectric phase transition of an improper character (I–II) at $T_1 \sim (486 \pm 1)$ K, a change in the conduction mechanism at (428 ± 2) K and a structural phase transition (II–III) at $T_2 \sim 345$ K.

The variation of ε″, the imaginary part of the dielectric permittivity, as a function of temperature, 95 K < T < 280 K is shown in Fig. 3a. The frequency range (1–10 kHz) has been only considered for the purposes of clarity.

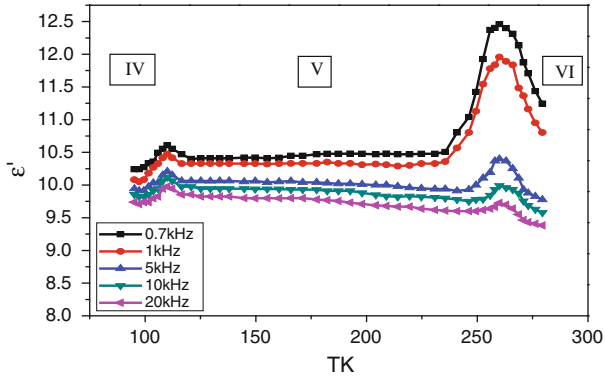

Fig. 2 Temperature dependence of the real part (ε′) of the dielectric permittivity measured at different frequencies for KIO_3

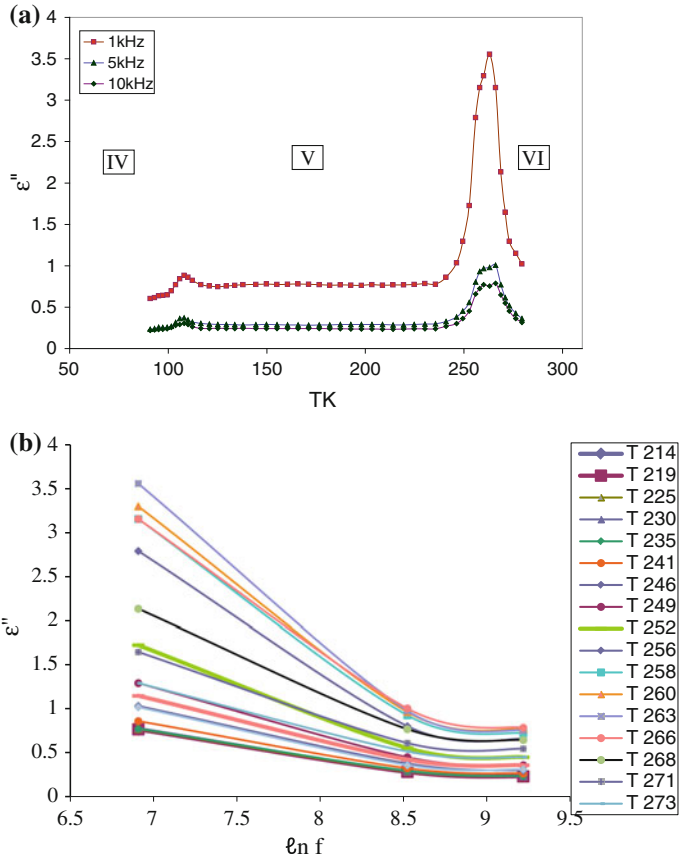

Fig. 3 **a** Temperature dependence of the imaginary part (ε″) of the dielectric permittivity measured at different frequencies for KIO_3. **b** Relation between ε″ versus ℓnf at different temperatures for KIO_3

Apparently, the general trend of this plot is similar to that of ε′-T graph, Fig. 2, except that the value of ε″ at a given frequency and temperature is much reduced as compared with the corresponding value of ε′, Fig. 2.

Figure 3b shows the frequency dependence of the imaginary ε″ plotted as ε″ versus ℓnf at some selected temperatures. The plot indicates that the dispersion increases with increasing temperature and decreasing frequency which is in agreement with the typical behavior of the dielectric materials.

The variation of the (dielectric loss), tan δ = ε′/ε″ as a function of temperature (95 K < T < 280 K) measured at some selected frequencies is shown in Fig. 4. The general trend of the plot indicates also the existence of two phase transitions at the above mentioned temperatures and are reflected as two peaks.

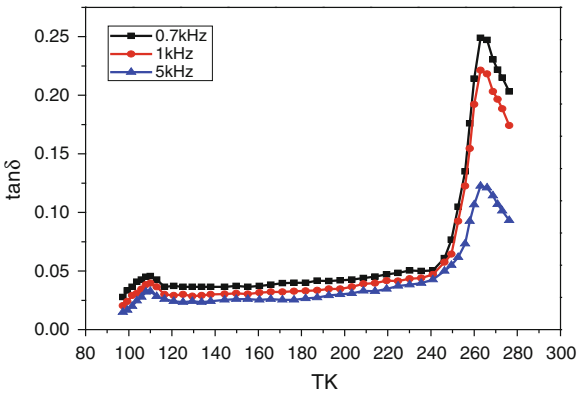

Fig. 4 Temperature dependence of tan δ measured at different frequencies for KIO_3

3.3 Electrical Conductivity

Obviously the conductivity depends on both, the temperature and the frequency.

3.3.1 Temperature Dependence

The ac conductivity $\sigma_{(\omega)}$ as function of temperature, 95 K < T < 280 K and frequency 0.7–20 kHz, plotted as $\ell n(\sigma T)$ versus 1/T is shown in Fig. 5. The behavior of σ seems to be in accordance of Arrhenius relation. For a given frequency, and as the temperature increases from about 95 K, the first broad peak is observed at ≈258 K. The other phase transition is found at ≈110 K. Between the two transition regions the behavior of σ obeys Arrhenius relation.

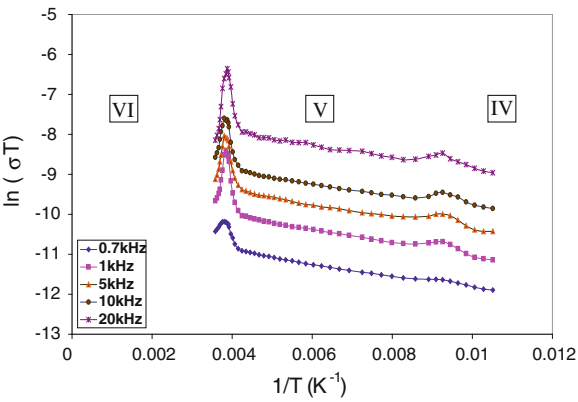

Fig. 5 Variation of ($\ell n\sigma$ T vs. 1/T) at different frequencies for KIO_3

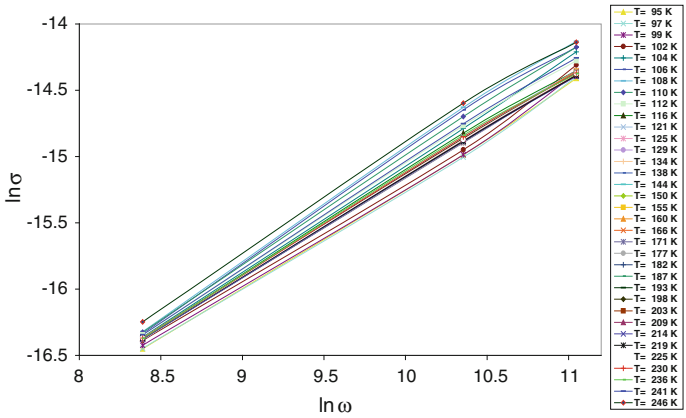

Fig. 6 Double logarithmic *plot* ($\ell n\sigma$ vs. $\ell n\omega$) for KIO_3

3.3.2 Frequency Dependence

The variation of $\ell n\sigma$ versus $\ell n\omega$ at different temperatures is shown in Fig. 6.

The plot is consists of a series of straight lines of different slopes. The slope of each line gives the value of s, where $s = \left(\frac{\partial \ln \sigma}{\partial \ln \omega}\right)_{T=const.}$ at that temperature. The temperature dependence of s is shown in Fig. 7. Apparently, s is practically temperature independent except for in the phase transition regions.

Figure 8 shows the variation of the pre-exponential factor (A) with temperature, plotted as ℓn A versus T. The behavior of the plot indicates also the existence of two phase transitions at the same mentioned temperatures (258 and 110 K) which are reflected in the graph shown as "inverted peaks".

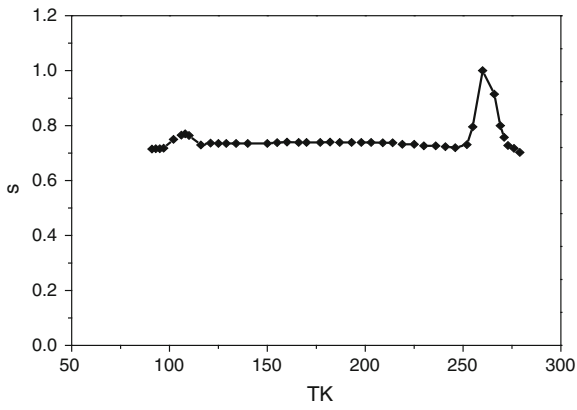

Fig. 7 Temperature dependence of the frequency exponent (s) for KIO_3

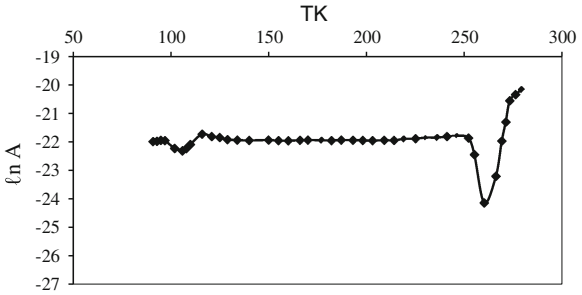

Fig. 8 Variation of ℓn A versus T for KIO_3

4 Discussion

The values of the transition temperatures T_3 (III–IV) = 258 K and T_4 (IV–-V) = 110 K of the present work was found to be consistent with those found by previous workers (Tables 1 and 2). For example, from his previous investigation of the ferroelectricity in KIO_3 single crystal, Salje [17] observed two phase transitions in the low-temperature region at ≈−15 °C (258 K) and at −163 °C (110 K).

Furthermore, Ivanov et al. [15] studied the temperature dependence of the optical axes angle 2v, the birefringence in the z-cut $\delta n_{(z)}$ and the spontaneous polarization axes P_{sf} in a wide temperature range and they observed that at T = −15 °C (258 K) all three curves [(2v (T), $\delta n_{(z)}$(T) and P_{sf} (T)] exhibit only breaks and thus they suggested that this transition is to be of a second order. Moreover, although Ivanov et al. [15] did not investigate the phase transition (IV–V) in detail, yet they observed a regular quantitative change of the domain pattern which confirms the existence of a transition with a lowering of point symmetry. Moreover, they demonstrated the existence of ferroelectricity in the compound at the liquid nitrogen temperature −195 °C (78 K) by observing the D-E hysteresis loops which was found to be clear at that temperature and thus they concluded that phase V behaves as a ferroelectric which is in a good agreement with the present work and also with the work of

Table 2 Summary of the crystal structure at some selected temperatures for the compound KIO_3

Temperature (K)	Crystal data	Technique	References
530	Rhombohedral, R3 m, Z = 1	High energy X-ray powder diffraction MEM/Reitveld analysis	[29]
523	Rhombohedral, R3, Z = 1	Neuton powder diffraction technique (Rietveld method)	[30]
Room temperature	Triclinic symmetry	Single crystal X-ray diffraction	[28]
523	Triclinic, P1, Z = 4	Neutron powder diffraction technique	[31]
300	Triclinic, P1, Z = 4	(Rietveld method)	[32]

Herlach [12], where the crystal remains ferroelectric below 485 K [12]. In somewhat recent work Maeda et al. [19] demonstrated the existence of low temperature phase transitions at $T_3 = -15$ °C (258 K) and $T_4 = -160$ °C (113 K). A similar behavior has been observed for NH_4IO_3 where the compound undergoes a ferroelectric phase transition at ≈368 K and behaves as a ferroelectric material below 368 K down to liquid nitrogen temperature [34].

Among other things, although some investigators have been reported on the low-temperature phase transitions in KIO_3, through the study of the temperature dependence of some parameters, yet, the only crystal structure of the low temperature is that determined by Lucas [32]. The data do not show significant change, on the atomic level, relative to that of the room temperature, i.e. no strong evidence for low temperature structural phase transitions. As we mentioned above, the temperature dependence of some properties show detectable change at ≈258 K and at ≈110 K. This inconsistence is not a major problem, since the structural phase transitions that involve only minor changes in atomic positions are not easy to detect [45]. Potassium chlorate $KClO_3$ represents an example of a crystal with a reported phase transition with very small structural change where the atomic arrangement and coordination above and below the phase transition are identical [45]. The same conclusion was also given by Brooker et al. [46]. From Raman studies of the phase transition in $KClO_3$, they observed that the difference in the vibrational spectra of the two phases was very small and hence the transition (at 545 K) involved only mainor rearrangement of the ClO_3 ion. Similar saturation may exist for the KIO_3 since the two compounds (KIO_3 and $KClO_3$) are members of halate series of the general molecular formula MXO_3 where (X = Cl, Br and I).

From the crystal structure point of view [29–31], the I and O atoms exist in the crystals as IO_3 molecules rather than the IO_6 complex. In other words unlike the typical perovskite structure of ABO_3 ferroelectrics where six O atoms form O_6 octahedron surrounding, a B atom each I atom in KIO_3 has three nearest O atoms forming an IO_3 molecule [26].

At this stage, it is necessary to mention that although there is a good agreement between different authors that the compound undergoes two phase transitions in the temperature interval $95\ K < T < 280\ K$, yet there is a discrepancy concerning the nature and/or the exact mechanism of these transitions. Some authors consider these transitions to be associated with the orientational glass transitions [19]. Other authors [46] proposed that these transitions might be associated with the structural changes of domain which is generally independent on atomic arrangements.

The present work tries to construct a bridge or link between different visions. The motion and/or the change of the structure of ferroelectric domains with temperature was first suggested by Byrom and Lucas [30]. On the other hand, and in a similar way to the role of ClO_3^- as the main cause of the structural phase transition in the $KClO_3$ compound, one cannot neglect the effect of the reorientational motion of the IO_3^-, since, as we mentioned above, the spatial correlation between IO_3^- decreases with increasing temperature [29]. Thus the thermal energy at each transition temperature may be enough to cause the change of the structure of ferroelectric domains

and at the same time initiate (stimulate) the orientational motion of the IO_3^- and hence a very slight rearrangement of the molecule with a very minor change in the atomic position in a way similar to that observed in the $KClO_3$ [45, 46].

It is of interest to mention here that even for the structural phase transition of the KIO_3 that have been observed at ~487 K which is associated with the ferroelectric phase transition, the two X-ray diffraction patterns above and below the mentioned transition temperature are very similar [30]. In our vision, the exact mechanism of the low temperature phase transition is a future problem and requires the use of the high energy X-ray (synchrotron) powder (and not single) technique which is beyond the scope of the present work.

For the problems of unsaturated D-E hysteresis loops shown in Fig. 1, it is known that the compound behaves as an "improper ferroelectric material" [20, 24–26] and not as (usual) ferroelectrics. The characteristic features of the improper ferroelectric are [47, 48]:

(i) a very slight change of dielectric constant near Tc
(ii) a low spontaneous polarization

Logically, the spontaneous polarization is not the order parameter and not proportional to it as in the case of proper ferroelectrics. The factor (ii) is the most responsible for the unsaturation in the D-E hysteresis loops. The case of KIO_3 is very similar to the improper ferroelectric NH_4IO_3 where the D-E hysteresis loops in the ferroelectric phase are also unsaturated [34, 49].

Regarding the charge transport mechanism in different phases, it is known that the three main processes that contribute significantly to the ac conductivity [37, 50, 51] are the quantum mechanical tunneling QMT, the correlated barrier hopping (CBH), and the small polaron tunneling (SPT).

For QMT model, the value of s is given by

$$s = 1 - \frac{4}{\ln\left(\frac{\upsilon_{ph}}{\omega}\right)} = 1 - \frac{4}{\ln\left(\frac{1}{\omega\tau}\right)} \tag{5}$$

whereas for (CBH) model, we have

$$s = 1 - \frac{6\,kT}{E_0 - \ln\left(\frac{\upsilon_{ph}}{\omega}\right)} = 1 - \frac{6\,kT}{E_0 - \ln\left(\frac{1}{\omega\tau}\right)} \tag{6}$$

and finally for the (SPT),

$$s = 1 - \frac{4}{\ln\left(\frac{1}{\omega\tau_p}\right) - w_H/kT}. \tag{7}$$

The symbols in (5), (6) and (7) take their conventional meanings where k is Boltzmann's constant, E_0 is the optical energy band, υ is the frequency of the

phonon. τ_p is the relaxation time of the polaron (of the order of 10^{-13} s) and w_H is the activation energy involved in the electron transfer process between a pair of states. Moreover, the value of s in (5) is temperature independent, whereas in (6) s decreases with increasing the temperature and is less dependent on the frequency. For SPT, (7) predicts that, s increases as T increases.

Referring to Fig. 7, where s is plotted as a function of temperature, it is clear that the value of s is practically temperature independent i.e. in accordance with (5). Thus, the QMT model is the most likely one in this range of temperature. Moreover, if we put υ_{ph} ($\sim 10^{-13}$ s^{-1} and $\omega \sim 10^4$ rad/s) [37] into (5), then the value of s $\sim$ 0.76, which is in a good agreement with our experimental value, Fig. 7.

Furthermore, for QMT model, the value of $\sigma(\omega)$ as given by Auston and Mott [52] and Efros [53] is

$$\sigma(\omega) = \frac{\eta}{3} e^2 kT \left[N(E_{f)(T)}\right]^2 \alpha^{-5} \omega \left[\ln\left(\frac{\upsilon_{ph}}{\omega}\right)\right]^4 \tag{8}$$

where:

e	is the charge of electron,
T	is the absolute temperature,
$N(E_f)$	is the density of energy states near the Fermi level,
α	is the electron wave function decay constant 1 Å [34],
υ_{ph}	is the phonon frequency, and
η	is a constant.

Equation (8) predicted that, there is a linear relation between ω and $\frac{\sigma(\omega)}{\left[\ln\left(\frac{\upsilon_{ph}}{\omega}\right)\right]^4}$ such a relation is presented in Fig. 9, which again confirm (8) where a series of almost straight lines of different slopes are observed. Thus the QMT model is the best one that describes the conduction mechanism in the investigated temperature region.

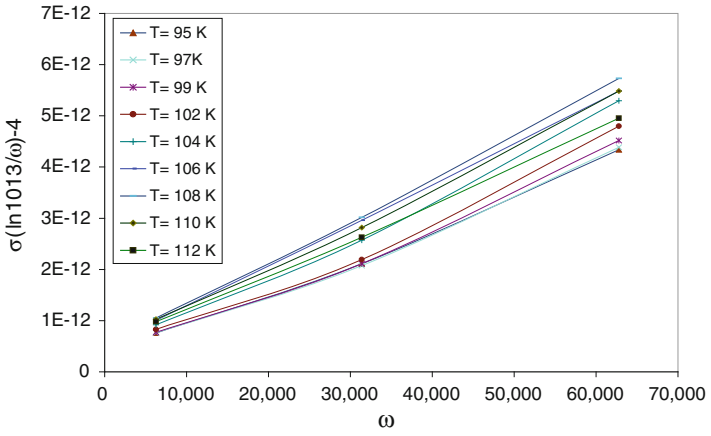

Fig. 9 Variation of σ(ω)/[ℓn(ʊph/ω)]4 versus ω at different temperatures for KIO_3

5 Conclusion

The present data indicate that in the investigated low temperature region 95 K < T < 280 K, the compound remains ferroelectric (of an improper character) where the ferroelectric hysteresis loops, of quite insufficient saturation, are observed clearly over the mentioned temperature intervals. This is also the case for the similar compound NH_4IO_3 where it undergoes a ferroelectric phase transition of an improper character at ≈368 K and remains ferroelectric down to liquid nitrogen temperature. For the compound KIO_3, the behavior of the temperature dependences of all electrical parameters confirms and supports each other and indicates clearly that compound undergoes two structural phase transitions at $T_3 \approx 258$ K and at $T_4 \approx 110$ K over the mentioned temperature range. It is known that the iodine and oxygen atoms in the present compound exist as IO_3 rather than as IO_6 complex and the spatial correlation between IO_3 becomes weak with increasing temperature. The thermal energy (kT) at the transition temperature is enough to cause the rearrangement of IO_3 molecules in a way similar to the case of $KClO_3$. The thermal energy also causes an observable change in the structure of ferroelectric domain.

Regarding the electrical conduction, in the investigated low temperature region, the QMT model seems to be the main mechanism for the charge transport. This is to be expected, since this model usually exists in the low temperature range.

The low and high phase transitions as well as the change in conduction mechanism at (428 ± 2)K are shown in the following scheme. The values of the transition temperatures are taken from [20] and the present work except for transition at T = 33 K is taken from [19].

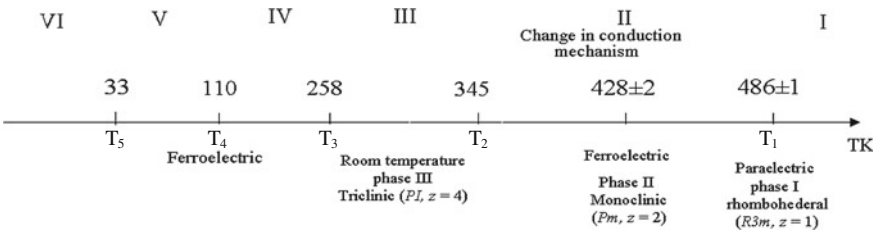

References

1. Barabash A, Gavrilko T, Eshimov K, Puchkovskaya G, Shanchuk A (1999) J Mol Struct 145:511–512
2. Bismayer U, Salje E, Viswanathan K (1979) Phase Transitions 1:35
3. Abdel-Kader MM, El Kabbany F, Naguib H, Gamal WM (2008) Phase Transitions 81:83
4. Colomban P (1992) Proton conductors, (Solids, membranes and gels materials and devices) Part I P.1. Cambridge University Press, Cambridge
5. Crettez JM, Righi A, Galez C, Bourson P, Mareira RL (1998) Solid State Commun 105:481
6. Gaffar MA, Abu El-Fadl JA (1999) J Phys Chem Solid 60:1633

7. Bergman JG, Boyd GD Jr, Ashiken A, S-Kurtz (1969) J Appl Phys 40:2860
8. Keve ET, Abrahams SC, Berustein JL (1971) J Chem Phys 54:2556
9. Kurtz SK, Perry TT (1965) Appl Phys Lett 12:156
10. Crane GR, Bergman JC, Glass AM (1969) J Am Ceram Soc 52:655
11. Helg H, Gruncher H (1970) J Phys Soc Jpn 28(Supl):169
12. Herlach F, Helv (1961) Helv Phys Acta 34:305
13. Salje E (1972) Z Krishtallagr 136:135
14. Crane GR (1972) J Appl Cryst 5:360
15. Ivanov NR, Shuvalov LA, Chikgladze OA (1973) Phys Lett 45A:437
16. Salje E (1971) Z Krishtallagr 134:107
17. Salje E (1974) Z Krishtallagr 139:317
18. Landolt Bornstein (1982) vol 111/16b. Springer, Berlin p 269
19. Maeda M, Takagi M, Suzuki I (2000) J Phys Soc Jpn 69:267
20. Abdel Kader MM, El-Kabbany F, Naguib HM, Gamal WM (2008) Phase Transitions 81:29
21. Filimonov AA, Survotov LG, Paklomov VS, Sonin AS (1965) Sov Phys Cryst 10:202
22. X- Yin, Lü MK (1992) Appl Phys Lett 60:2849
23. Haussühl S, Jyang W, Mengkai LÜ (1995) Cryst Res Technol 30:535
24. Ahart M, Kojam S, Takagi M, Maeda M, Suzuki I (1998) Jpn J Appl Phys 37:5687
25. Loiacono GM, Jacco JG (1985) Mater Lett 4:27
26. Liu L, Wu RQ, Ni ZH, Shen ZX, Feng YP (2006) J Phys Conf Ser 28:105 (and references there in)
27. Hamid SA (1973) Z Kristallogr 137:412
28. Kalinin VR, Llyukhin VV, Belov NV (1978) Sov Phys Dokl 12:1978
29. Kasatani H, Aoyagi S, Kuroiwa Y, Yagi K, Katayama R, Terauchi H (2003) Nucl Instr Meth B 199:49
30. Byrom PG, Lucas BW (1987) Acta Crystallogr C 43:1651
31. Lucas BW (1984) Acta Crystallogr C 40:1989
32. Lucas BW (1985) Acta Crystallogr C 41:1388
33. Bajsa DF, Barabash AI, Vertegel IG (1981) Ukr Fiz Zhurnal 10:1745
34. Abdel Kader MM, El-Kabbany F, Naguib HM, Gamal WM (2013) Phase Transit 36:947–958
35. Jonsher AK (1983) Dielectric relaxation in solids. Chelsea Dielectric press, London, p 223
36. Dyre JC (1988) J Appl Phys 64:2456
37. Elliott SR (1987) Adv Phys 36:135
38. Krthik C, Varma KBR (2006) J Phys Chem Sol 67:2437
39. Louati B, Gargouri M, Guidara K, Mhiri T (2005) J Phys Chem Sol 66:762
40. Dyre JC, Schroder TB (2000) Rev Mod Phys 72:873
41. Chen RH, Yen Chen-Chief, SHern CS, Fukami T (2006) Sol State Ion 177:2857
42. Lee WK, Liu JF, Nowick AS (1991) Phys Rev Lett 67:1559
43. Moawad HMM, Jain H, El-Mallawany R (2009) J Phys Chem Sol 70:224
44. Al Refaie SN, El-Rayyan HSB (1992) J Mater Sci Lett 11:958
45. Ramachandran N, Lonappan MA (1957) Acta Cryst 10:281
46. Brooker MH, Shapter JG (1989) J Phys Chem Solids 50:1087
47. Blinc R, Zekz B (1974) Soft modes in ferroelectrics and antiferroelctrics. North-Holand Publishing company, Amsterdam, pp 15, 45
48. Astrukov B, Levanyuk AP (1998) Ferroelectric phenomena in crystals. Springer, Berlin, p 74
49. Oka T, Mitsui T, Sawada S (1976) J Phys Soc Jpn 40:913
50. Gamati F, Fattoum A, Bohli N, Dhaoui W, Mohamed AB (2007) J Phys: Condens Matter 19:36203
51. Long AR (1982) Adv Phys 31:553
52. Austin IG, Mott NF (1969) Adv Phys 18:41
53. Efros AL (1981) Phillos Mag 43:829